

Cronin effect from backward to forward rapidity: a tale of two misteries.

Alberto Accardi

Columbia University, Department of Physics
538 West 120th Street, New York, NY 10027, USA

Received May 15th, 2004

Abstract. I discuss recent experimental data on the Cronin effect in deuteron-gold collisions at the top RHIC energy, in a pseudorapidity range $\eta \in [-2, 3]$. Two theoretical approaches are compared and contrasted: the pQCD-based Glauber-Eikonal model and Colour Glass Condensate models. Neither can describe the Cronin effect over the whole pseudorapidity interval up to now explored experimentally, its most mysterious and intriguing part being at negative rapidity.

Keywords: Cronin effect, pQCD, CGC, p+A collisions

PACS: 12.38.Mh; 24.85.+p; 25.75.-q

In hadron-nucleus ($p + A$) and nucleus-nucleus ($A + A$) collisions at relativistic energy the hadron transverse momentum spectra at moderate $p_T \sim 2-6$ GeV are enhanced relative to linear extrapolation from $p + p$ reactions. This ‘‘Cronin effect’’ has been observed on an energy range $\sqrt{s} \approx 20 - 200$ GeV in both $p + A$ and $A + A$ collisions [1]. It is generally attributed to multiple scattering of projectile partons propagating through the target nucleus [2], and is a sensitive probe of initial-state modifications of the nuclear wave function ($p + A$ collisions) and of final state in-medium effects ($A + A$ collision) [3]. The Cronin effect may be quantified by taking the hadron p_T spectrum in $p + A$ collision in a given centrality class (*c.cl.*), normalizing it to binary scaled $p + p$ collisions by the inverse thickness function T_A , and finally dividing it by the $p + p$ spectrum:

$$R_{pA} = \frac{1}{T_A(c.cl.)} \frac{dN^{pA \rightarrow hX}}{dq_T^2 dy}(c.cl.) \bigg/ \frac{d\sigma^{pp \rightarrow hX}}{dq_T^2 dy}. \quad (1)$$

To cancel systematic errors as much as possible, it is also customary to take the ratio R_{cp} of a given centrality class to the most peripheral one.

1. Recent experimental results at RHIC

The BRAHMS results [4] on charged hadron R_{cp} in $d + Au$ collisions at $\sqrt{s} = 200$ GeV A in a rapidity range $\eta = 0 - 3.2$ are shown in Fig. 1, top panel. Two features are apparent. First, the Cronin peak at $p_T \simeq 3$ GeV in the mid-rapidity bin is progressively suppressed. At $\eta \gtrsim 2$, R_{cp} is always smaller than 1, tending to a plateau at larger transverse momenta. Second, the centrality dependence of the effect is reversed going from mid- to forward rapidity.

Peripheral collisions are expected to behave similarly to $p + p$ collisions: the more peripheral the collision, the thinner the nucleus, the smaller the rescattering probability. Therefore, the R_{cp} ratio should behave similarly to R_{dAu} . Quite strikingly, this is not the case, as shown in Fig. 1, bottom panel. The peak in R_{dAu} is suppressed in going from $\eta = 0$ to $\eta = 1$, as confirmed also by PHOBOS data [5], and looks similar to R_{cp} . However, at $\eta > 2$ the suppression doesn't seem to continue. Instead, the data grow quite rapidly toward 1, which is reached at $p_T \simeq 2$ GeV, and possibly stay close to 1 at higher p_T though experimental errors are too large to have a final say. This discrepancy is a mystery which cannot be explained up to now by current theoretical models, and needs further experimental investigation.

The second and most interesting mystery appears when we look at negative rapidities, i.e., at the Au side. Fig. 2, compiled by A.Purwar [6], presents a summary plot of the pseudorapidity dependence of the Cronin effect for charged hadrons

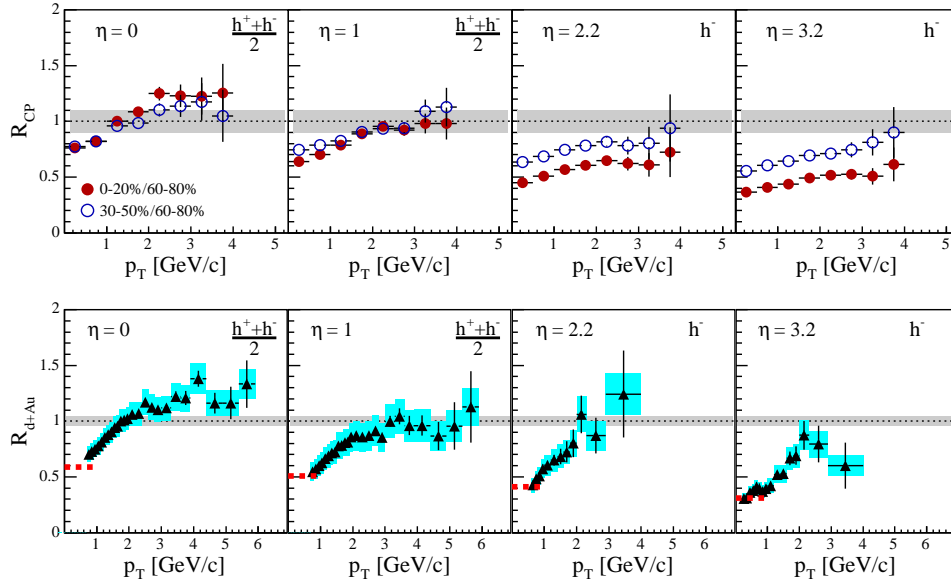


Fig. 1. Top: R_{cp} measured by BRAHMS [4] at rapidity $\eta \in [0, 3.2]$ for 2 centrality classes. **Bottom:** R_{dAu} in minimum bias collisions, measured by BRAHMS [4] at rapidity $\eta \in [0, 3.2]$. Note the striking difference of the forward rapidity R_{dAu} and R_{cp} .

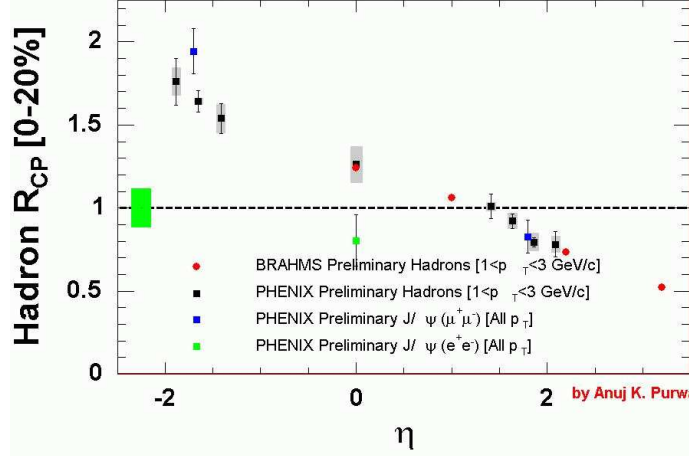


Fig. 2. Summary plot of preliminary results from PHENIX and BRAHMS for integrated R_{cp} at $1 < p_T \leq 3$ GeV. Figure from Ref. [6].

integrated on $1 < p_T < 3$ GeV. As the rapidity decreases, the gold Bjorken's x increases. Then, the parton densities probed by the deuteron decrease and one would naively expect multiple scatterings and the Cronin effect to decrease, so that R_{cp} should tend to 1. On the contrary, experimental data show a steady increase as η decreases, reaching $R_{cp} \sim 1.8$ at $\eta = -2$. This large value cannot be accounted for by standard nuclear effects like anti-shadowing [7], or non perturbative string fragmentation which pulls hadron production slightly toward the Au side [8]. Moreover, the same trend at negative η appears also in J/ψ production, ruling out a meson/baryon effect.

2. pQCD and Glauber-Eikonal models

The Glauber-Eikonal (GE) approach [9] to the Cronin effect treats multiple $2 \rightarrow 2$ partonic collisions in collinearly factorized pQCD, see Fig. 6, left panel. The low- p_T spectra in $p + A$ collisions are suppressed by unitarity. At moderate p_T , the accumulation of transverse momentum leads to an enhancement of transverse spectra. At high p_T the binary scaled $p + p$ spectrum is recovered: no high- p_T shadowing is predicted in this approach.

The cross-section for production of a parton of flavour i , with transverse momentum p_T and rapidity y in $p + A$ collisions at fixed impact parameter b , is written as

$$\frac{d\sigma^{pA \rightarrow iX}}{d^2p_T dy d^2b} = \langle x f_{i/p} \rangle_{y_i, p_T} \frac{d\sigma^{iA}}{d^2p_T dy_i d^2b} \Big|_{y_i=y} + T_A(b) \sum_b \langle x f_{i/A} \rangle_{y_i, p_T} \frac{d\sigma^{ip}}{d^2p_T dy_i} \Big|_{y_i=-y} \quad (2)$$

where where $T_A(b)$ is the target nucleus thickness function. Hadron spectra are then obtained as a convolution with the appropriate fragmentation function $D_{i \rightarrow h}(z, Q)$.

The first term in Eq. (2) accounts for multiple semihard scatterings of the parton i on the target nucleus; in the second term the nucleus partons are assumed to undergo a single scattering on the proton. The average parton flux from the proton, $\langle x f_{i/p} \rangle$, and the parton-nucleon cross-section, $d\sigma^{iN}$, are defined as

$$\begin{aligned} \langle x f_{i/p} \rangle_{y_i, p_T} &= \frac{K}{\pi} \sum_j \frac{1}{1 + \delta_{ij}} \int dy_2 x_1 f_{i/p}(x_1, Q^2) \frac{d\hat{\sigma}^{ij}}{d\hat{t}} x_2 f_{j/N}(x_2, Q^2) \bigg/ \frac{d\sigma^{iN}}{d^2 p_T dy_i} \\ \frac{d\sigma^{iN}}{d^2 p_T dy_i} &= \frac{K}{\pi} \sum_j \frac{1}{1 + \delta_{ij}} \int dy_2 \frac{d\hat{\sigma}^{ij}}{d\hat{t}} x_2 f_{j/N}(x_2, Q^2) \end{aligned} \quad (3)$$

where \hat{t} is the Mandelstam variable and $d\hat{\sigma}/d\hat{t}$ are leading order parton-parton cross-sections in collinearly factorized pQCD. K is a constant factor which takes into account next-to-leading order corrections. To regularize the IR divergences of the single-scattering pQCD parton-nucleon cross-sections a small mass regulator p_0 is introduced in the propagators, and $Q = \sqrt{p_T^2 + p_0^2}/2$ is the scale of the hard process. Finally, we introduce a small intrinsic transverse momentum $\langle k_T^2 \rangle = 0.52$ GeV² to better describe the hadron spectra in $p+p$ collisions at intermediate $p_T=1-5$ GeV. The free parameters p_0 and K in Eqs. (3) are fitted to hadron production data in $p+p$ collisions at the energy and rapidity of interest. This allows to compute the spectra in $p+A$ collision and the Cronin ratio with no extra freedom. For more details, see Ref. [9].

Nuclear effects are included in $d\sigma^{iA}$, the average transverse momentum distribution of a proton parton who suffered at least one semihard scattering:

$$\begin{aligned} \frac{d\sigma^{iA}}{d^2 p_T dy d^2 b} &= \sum_{n=1}^{\infty} \frac{1}{n!} \int d^2 b d^2 k_1 \dots d^2 k_n \delta\left(\sum_{i=1,n} \vec{k}_i - \vec{p}_T\right) \\ &\quad \times \frac{d\sigma^{iN}}{d^2 k_1} T_A(b) \times \dots \times \frac{d\sigma^{iN}}{d^2 k_n} T_A(b) e^{-\sigma^{iN}(p_0)T_A(b)}. \end{aligned} \quad (4)$$

This equation resums all processes with n multiple $2 \rightarrow 2$ parton scatterings. The exponential factor in Eq. (4) represents the probability that the parton suffered no semihard scatterings after the n -th one, and explicitly unitarize the cross-section at the nuclear level. Unitarity introduces a suppression of parton yields compared to the binary scaled $p+p$ case. This is best seen integrating Eq. (4) over the transverse momentum: $d\sigma^{iA}/dy d^2 b \approx 1 - e^{-\sigma^{iN}(p_0)T_A(b)}$. At low opacity $\chi = \sigma^{iN}(p_0)T_A(b) \ll 1$, i.e., when the number of scatterings per parton is small, the binary scaling is recovered. However, at large opacity, $\chi \gtrsim 1$, the parton yield is suppressed: $d\sigma^{iA}/dy d^2 b \ll 1 < \sigma^{iN}(p_0)T_A(b)$. This suppression is what we call “geometrical shadowing”, since it is driven purely by the geometry of the collision through the thickness function T_A . As the integrated yield is dominated by small momentum partons, geometrical shadowing is dominant at low p_T . Beside the geometrical quark and gluon shadowing, which is automatically included in GE

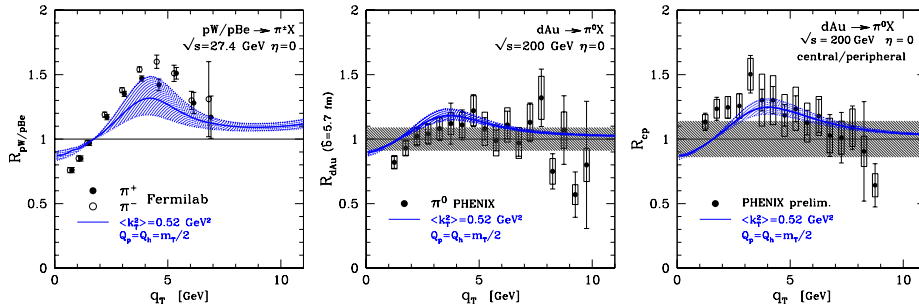


Fig. 3. Cronin effect on pion production at Fermilab [10] and RHIC [11] at $\eta = 0$. The solid curve is the GE computation. Theoretical errors due to the fit of p_0 are shown as a shaded band around the solid curve. The rightmost panel shows the 0-20%/60-88% centrality classes ratio.

models, at low enough x one expects genuine dynamical shadowing due to non-linear gluon interactions as described in, e.g., Colour Glass Condensate (CGC) models, see Section 3.

The GE model reproduces quite well both Fermilab and PHENIX data at $\eta = 0$ (Fig. 3 left and middle). It also describe the increase of the Cronin effect with increasing centrality (Fig. 3, right). The agreement of GE calculations with $y = 0$ data, and especially the centrality dependence, suggest that there is no dynamical shadowing nor CGC at RHIC midrapidity.

To address the BRAHMS data at forward rapidity $\eta \approx 3.2$ [4], we would first need to fit p_0 and K in $p + p$ collisions at the same pseudo-rapidity. Unfortunately the available p_T -range $p_T \lesssim 4$ GeV is not large enough for the fit to be done. Therefore, we use the parameters extracted at $\eta = 0$. The resulting Cronin ratio, shown by the solid line in Figure 2, overestimates the data at such low- p_T . However, the opacity $\chi_0 = 0.95$ might be underestimated, due to the use of the mid-rapidity parameters. To check this we tripled the opacity: the resulting dashed line touches the data at $p_T \gtrsim 2$ GeV, but predicts a strong Cronin peak at $p_T \gtrsim 3$ GeV. On the other hand, a similar strong peak would appear in the computation of R_{cp} , in contrast with the data in Fig. 1.

3. Colour Glass Condensate models

The Colour Glass Condensate (CGC) is an effective theory for the nuclear gluon field at small- x [12]. The valence quarks, treated as a collection of random colour sources ρ , radiate the gluon field A . At low- x the gluon occupation number is so large that the gluon field can be treated semi-classically and computed as a solution of Yang-Mills equation of motion in the presence of colour sources. The theory is characterized by a saturation scale Q_s . Gluons with momenta lower than this scale are in the “saturation” regime: their density is so high that gluon-gluon fusion processes limit a further growth. At large momenta the gluon field is in the perturbative “parton gas” regime. A recently conjectured intermediate “geometric

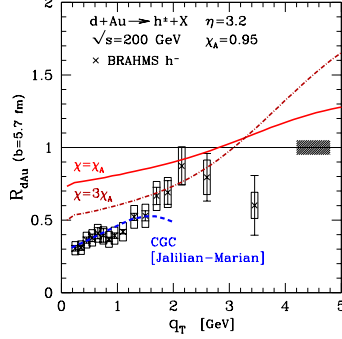


Fig. 4. Cronin ratio at $\eta = 3.2$. The solid and dot-dashed curves are the GE model computation with $\chi = \chi_0$ and $\chi = 3\chi_0$, respectively. The dashed curve is a CGC computation by Jalilian-Marian [16]. Data are taken from [4].

scaling window” may extend at momenta $Q_s < p_T < Q_s^2/Q_0$, where quantum effects from the saturation region further modify the evolution from the perturbative to the saturation region.

Observables $\mathcal{O}[A[\rho]]$ are computed as an average over the colour sources with a weight $W_y[\rho]$ depending on the gluon rapidity $y = \log(1/x)$ as follows: $\langle \mathcal{O}[A] \rangle_y = \int D\rho W_y[\rho] \mathcal{O}[A[\rho]]$. Gluons at a given x are themselves colour sources for gluons at smaller $x' < x$. This evolution of the gluon field with x is captured by the so-called JIMWLK evolution equation [12].

If one approximates the proton as a dilute colour source, gluon production in $p + A$ collisions can be explicitly written in a k_T -factorized form [13]:

$$\frac{d\bar{N}_g}{d^2\mathbf{q}_\perp dy} = \frac{1}{16\pi^3 q_\perp^2} \int \frac{d^2\mathbf{k}_\perp}{(2\pi)^2} \varphi_p(\mathbf{q}_\perp - \mathbf{k}_\perp) \left[k_\perp^2 \int d^2\mathbf{r}_\perp e^{i\mathbf{k}_\perp \cdot \mathbf{x}_\perp} \langle U^\dagger(0)U(\mathbf{x}_\perp) \rangle \right].$$

Here, the proton’s unintegrated wave function φ_p is multiplied by the squared scattering amplitude on the target nucleus, expressed as a correlator of two Wilson lines. When the weight W is Gaussian,

$$W_y[\rho] = \mathcal{N}_y \exp \left[\frac{1}{2} \int_{-\infty}^y dy \int d\mathbf{x}_\perp d\mathbf{y}_\perp \frac{\rho^a(\mathbf{x}_\perp) \rho^a(\mathbf{y}_\perp)}{\lambda_y(x_\perp - y_\perp)} \right],$$

gluon production in $p + A$ collision can be interpreted as multiple $2 \rightarrow 1$ partonic scatterings as illustrated in Fig. 6, center.

To proceed further, one needs to choose a specific model for the colour sources. The McLerran-Venugopalan model assumes the gluon correlations to be local: $\lambda(\mathbf{x}_\perp - \mathbf{y}_\perp) = Q_s(x) \delta(\mathbf{x}_\perp - \mathbf{y}_\perp)$ where $Q_s(x) = \alpha_s^2 \frac{8\pi N_c}{N_c - 1} x G(x, Q^2)$. Quantum evolution of the gluon field is included naively in the x -dependence of Q_s only. An estimate from Ref. [13] of the Cronin effect on gluon production is presented in Fig. 5, left. It qualitatively agrees with experimental data at $y = 0$. However, at $y = 3$ it predicts a rightward shift and an increase of the Cronin peak (analogously to the GE model). It is disfavored by the R_{cp} data, though not incompatible with R_{dAu} .

On the other hand, at larger rapidities (i.e., at small x) the system undergoes a long quantum evolution, and enters the saturation regime. Thus, we should solve the JIMWLK equation. In the Gaussian approximation, a self-consistent solution

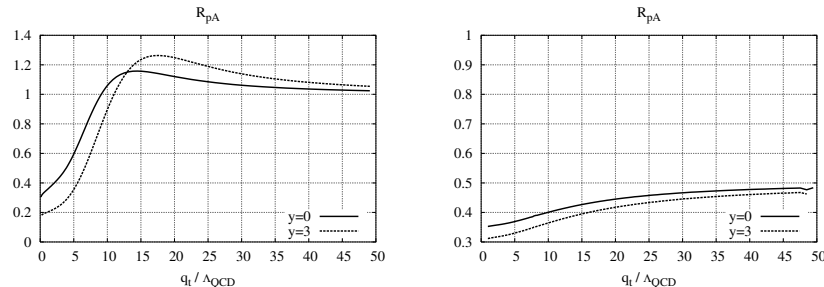


Fig. 5. Cronin effect in the MV model with naive quantum evolution (left) and with full evolution in the “deep saturation” limit (right). Figure taken from Ref. [13].

in the saturation regime exists, but with non-local gluon correlations [14]. In other words, the gluon density has become so high that gluons are no more bound to single nucleons, but correlate over macroscopic distances. The resulting Cronin ratio is highly suppressed over the whole p_T range, in qualitative agreement with $R_{cp}(y = 3)$. However, it disagrees both with the forward $R_{dAu}(y = 3)$ and with mid-rapidity data.

A word of caution: at large η valence quark production is important, if not dominant, as demonstrated by the excess of positively charged hadrons over negatively charged ones in $p + p$ collisions at $\eta = 3.2$ and $p_T > 2$ GeV [15]. Therefore, these computations should be considered only as illustrative of the physics included in the CGC approach. However, even the more quantitative computation of Ref. [16], who takes into account valence quarks and their fragmentation into charged hadrons, fails to reproduce the $p_T > 1.5$ GeV of R_{dAu} at $y = 3$, see Fig. 4¹.

4. Where does pQCD meet the CGC?

At mid-rapidity, GE and CGC models give similar results for the Cronin effect. Does this mean that to some extent they are equivalent, even if GE models describe multiple $2 \rightarrow 2$ scatterings and CGC multiple $2 \rightarrow 1$ scatterings? The standard answer is yes. Consider the single scattering terms depicted in Fig. 6, right. The single-inclusive cross section in pQCD is obtained by integration over the unobserved parton rapidity y' . In the limit of large $p_T \gg Q_s$ and asymptotic energy $p_T / \sqrt{s} e^{-y} \ll 1$, one obtains in the MV model $d\sigma_{pQCD} \approx d\sigma_{pQCD} \propto 1/p_T^4$ [18]. This is usually read as a proof that the single-inclusive cross section in the MV model reduces to pQCD in the high- p_T limit. Hence the GE and the MV models are equivalent.

However, the above equivalence can hold only in a restricted kinematic domain. This is clearly seen if we compute the average Bjorken’s x ’s probed in $p+p$ collisions. In the $2 \rightarrow 2$ kinematics, they depend on the rapidity of both the observed and the

¹A very recent computation [17] was more successful. It is based on a parametrization of the onset and rapidity dependence of quantum evolution which mimics CGC effects, and models valence quark scatterings in a different way than in Ref. [16].

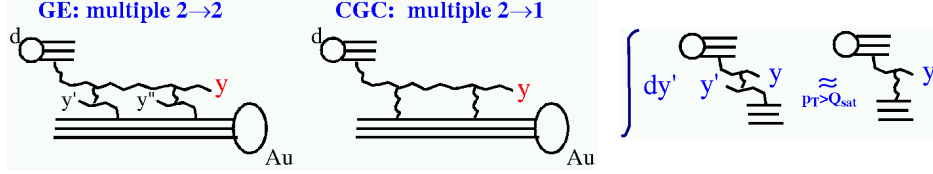


Fig. 6. *Left and middle:* Multiple scattering processes included in the GE and CGC models, respectively. *Right:* Illustration of the equivalence of pQCD and the MV model at high p_T discussed in Ref. [18].

unobserved parton:

$$x_{1,2}^{2 \rightarrow 2} = \frac{p_T}{\sqrt{s}} (e^{\pm y} + e^{\pm y'}) .$$

In $2 \rightarrow 1$ parton processes, the observed particle fixes them completely:

$$x_{1,2}^{2 \rightarrow 1} = \frac{p_T}{\sqrt{s}} (e^{\pm y}) .$$

As shown in Fig. 7, the $2 \rightarrow 1$ and $2 \rightarrow 2$ processes probe the target at quite different Bjorken's x ! The reason of this difference is that in the $2 \rightarrow 2$ processes one has to integrate over the unobserved particle, over a quite large phase space $\Delta y' \approx 10$. When y is large, most of these particles are produced at small or negative rapidity, which compensate the decrease in $\langle x_2 \rangle$ expected when the rapidity of the observed particle increases.

Given Fig. 7, one is tempted to ask “Which of the two models is wrong: GE or CGC?” In my opinion, this is the wrong question. The existence of $2 \rightarrow 2$ hard scattering processes at mid-rapidity has been experimentally proved by the observation of back-to-back hadrons at large p_T in $p + p$ and $p + A$ collisions [21]. On the other hand, there is no reason to doubt about the existence of $2 \rightarrow 1$ processes. So a more pertinent question is “What is the interplay between $2 \rightarrow 2$ and $2 \rightarrow 1$ processes? Is there a region where one is dominant over the other?”

We may have a clue at the answer from the following zeroth-order argument. Neglecting the quarks for ease of notation, the single inclusive cross-section for $2 \rightarrow 2$ processes may be evaluated as:

$$\begin{aligned} \frac{d\sigma^{pp \rightarrow gX}}{dy} &= \int dy' x_1 G(x_1) x_2 G(x_2) \frac{d\hat{\sigma}}{d\hat{t}} \\ &\approx \Delta y' \times xG(\langle x_1 \rangle_{2 \rightarrow 2}) xG(\langle x_2 \rangle_{2 \rightarrow 2}) \frac{d\hat{\sigma}}{d\hat{t}} \end{aligned}$$

where $\Delta y'$ is the width of the integration interval over y' , and $\langle x_{1,2} \rangle_{2 \rightarrow 2}$ can be read off Fig. 7. In the $2 \rightarrow 1$ case we have:

$$\frac{d\sigma^{pp \rightarrow gX}}{dy} \approx xG(\langle x_1 \rangle_{2 \rightarrow 1}) xG(\langle x_2 \rangle_{2 \rightarrow 1}) \frac{d\hat{\sigma}}{d\hat{t}}$$

where the value of $\langle x_{1,2} \rangle_{2 \rightarrow 1}$ is shown in Fig. 7. At mid-rapidity, $\langle x_2 \rangle_{2 \rightarrow 1} \approx \langle x_2 \rangle_{2 \rightarrow 2}$, then $2 \rightarrow 2$ processes are dominant because of a larger phase-space ($\Delta y' \approx 10$). At

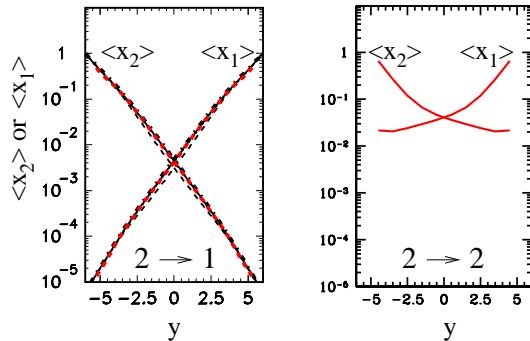


Fig. 7. Average $\langle x_1 \rangle$ and $\langle x_2 \rangle$ in $p+p$ collisions at RHIC energy, for $2 \rightarrow 1$ processes (left, taken from Ref. [20]) and $2 \rightarrow 2$ processes (right).

very forward rapidity, $\langle x_2 \rangle_{2 \rightarrow 1} \ll \langle x_2 \rangle_{2 \rightarrow 2}$; hence, $2 \rightarrow 1$ processes are dominant because of the small- x growth of parton distributions (the same argument can be used to analyze backward rapidities).

The transition between these two regimes is poorly known even in $p+p$ collisions, and should be more carefully studied, both theoretically and experimentally. This requires a formalism which is able to describe both processes in a unified framework. Collinear factorized pQCD is not suited, as kinematics forbids $2 \rightarrow 1$ processes if incoming partons have zero transverse momentum. On the other hand, k_T factorization can describe $2 \rightarrow 1$ processes, and the possible production of a second or more hard particles is hidden in the unintegrated distribution functions for the incoming partons [19, 20]. It is thus very suited for the problem at hand.

5. Conclusions

The pQCD based GE model is able to quantitatively describe the Cronin effect at midrapidity over a broad $\sqrt{s} = 20\text{--}200$ GeV energy range, indicating absence of CGC. However, at large rapidity it predicts an increasing Cronin effect, which is unfavoured by experimental data. Only incoherent $2 \rightarrow 2$ multiple parton scatterings are included in the GE model; adding coherence effects would suppress the Cronin peak, but still predict $R_{dAu} \sim R_{cp} \sim 1$ at large p_T [22]. On the other hand, CGC models describe $2 \rightarrow 1$ multiple coherent parton scatterings, and suggest at RHIC a transition from a non saturated region at mid-rapidity, to a saturated region at forward rapidity. Here, nonlocal gluon correlations created during quantum evolution suppress below 1 the otherwise increasing Cronin ratio. This predicted plateau at high- p_T is the hallmark of CGC. Unfortunately, the discrepancy between R_{dAu} and R_{cp} BRAHMS data, which is not present in any of the discussed models, does not allow to conclude whether this picture is correct or not.

At mid-rapidity GE and CGC models are usually thought to be equivalent, even though they describe different partonic subprocesses, and probe quite different Bjorken x 's at forward and backward rapidity. Simple kinematic considerations suggest a dominance of $2 \rightarrow 2$ processes at mid-rapidity, and of $2 \rightarrow 1$ processes at forward and backward rapidity. The interplay and transition between the two is poorly known, and needs to be studied more accurately already at the $p+p$ level,

then extended to $p + A$ collisions. The appropriate tools are already on the market: k_T -factorized pQCD on the theory side, and the STAR and PHENIX detectors on the experimental side. Azimuthal two-hadron correlations and their rapidity dependence are an especially suited observable for this purpose.

The steep increase of R_{cp} at negative rapidity adds a new dimension to the problem. Indeed both GE and CGC models expect the Cronin effect to be more and more reduced at $\eta < 0$. This is due to the decrease of the nucleus opacity $\chi_A(y)$ in one case, and of the saturation scale $Q_s(y) \propto e^y$ in the other. Standard nuclear effects like anti-shadowing are too weak to explain the magnitude of the negative rapidity Cronin effect, which requires a new theoretical explanation: either a neglected effect in the GE and CGC models, or a new piece of physics.

Acknowledgements. I would like to thank M.Gyulassy, P.Levai, A.Purwar, J.W.Qiu, A.Szczurek and X.N.Wang for inspiring discussions.

References

1. J. W. Cronin *et al.*, *Phys. Rev. D* **11** (1975) 3105. C. Klein-Boesing [PHENIX], talk at Quark Matter 2004 [arXiv:nucl-ex/0403024].
2. A. Accardi, in CERN Yellow Report on Hard Probes in Heavy Ion Collisions at the LHC [arXiv:hep-ph/0212148], and references therein.
3. M. Gyulassy and L. McLerran, arXiv:nucl-th/0405013.
4. I. Arsene *et al.* [BRAHMS], arXiv:nucl-ex/0403005.
5. G. Veres, talk at Quark Matter 2004, and these proceedings.
6. A. Purwar, poster at Quark Matter 2004, and seminar at Columbia University, Feb. 27th, 2004; M. X. Liu [PHENIX], arXiv:nucl-ex/0403047.
7. K. J. Eskola *et al.*, in CERN Yellow Report on Hard Probes in Heavy Ion Collisions at the LHC [arXiv:hep-ph/0302170].
8. X. N. Wang, *Phys. Lett. B* **565** (2003) 116
9. A. Accardi and M. Gyulassy, *Phys. Lett. B* **586** (2004) 244, and talk at Quark Matter 2004 [arXiv:nucl-th/0402101].
10. P. B. Straub *et al.*, *Phys. Rev. Lett.* **68** (1992) 452.
11. S. S. Adler *et al.* [PHENIX], *Phys. Rev. Lett.* **91** (2003) 072303.
12. E. Iancu, A. Leonidov and L. McLerran, arXiv:hep-ph/0202270.
13. J. P. Blaizot, F. Gelis and R. Venugopalan, arXiv:hep-ph/0402256.
14. E. Iancu, K. Itakura and L. McLerran, *Nucl. Phys. A* **724** (2003) 181.
15. R. Debbe [BRAHMS], arXiv:nucl-ex/0403052.
16. J. Jalilian-Marian, arXiv:nucl-th/0402080.
17. D. Kharzeev, Y. V. Kovchegov and K. Tuchin, arXiv:hep-ph/0405045.
18. M. Gyulassy and L. D. McLerran, *Phys. Rev. C* **56**, 2219 (1997).
19. B. Andersson *et al.* [Small x Collaboration], *Eur. Phys. J. C* **25**, 77 (2002).
20. A. Szczurek, *Acta Phys. Polon. B* **35** (2004) 161, and these proceedings.
21. J. Adams *et al.* [STAR], *Phys. Rev. Lett.* **91** (2003) 072304; G. Rakness [STAR], talk at the "RHIC & AGS Users' Meeting", BNL, May 10-14, 2004.
22. J. Qiu and I. Vitev, arXiv:hep-ph/0405068.